

# Multidetector CT Imaging of Coronary Artery Stents: Is This Method Ready for Use?

Jung Im Jung, MD

Department of Radiology, St. Mary's Hospital, College of Medicine, The Catholic University of Korea, Seoul, Korea

## ABSTRACT

Coronary artery stenting has become the most important nonsurgical treatment for coronary artery disease. However, in-stent restenosis occurs at a relatively high rate and this problem has led to the routine use of invasive angiography for assessing stent patency. Although coronary angiography is the clinical gold standard and it is a very effective diagnostic tool for detecting such in-stent restenosis, it's clearly an invasive procedure with its associated morbidity and mortality risks. Therefore, a noninvasive technique for detecting in-stent restenosis would be of great interest and use for following up patients after coronary angioplasty. Multidetector-row CT (MDCT) is being increasingly used for noninvasive coronary artery imaging as it has high diagnostic accuracy for detecting coronary artery stenosis in native, non-stented, coronary arteries. However, the application of MDCT to stent imaging is somewhat difficult. It is generally accepted that visualizing the in-stent lumen with using 4-slice MDCT is impossible because of the modality's low temporal and spatial resolution. There is increased visualization of the stent lumen on 16-slice MDCT, and so in-stent restenosis can be detected in assessable stents. Yet for stents with small diameters (<3 mm) and/or thicker struts, visualization of in-stent stenosis remains a problem. The recently introduced 64-slice CT offers more improved spatial and temporal resolution than does 16-slice CT and this results in superior visualization of the stent lumen and in-stent restenosis. However, although 64-slice MDCT allows for improved stent visualization, a relevant part (up to 47%) of the stent lumen is still not assessable. There are many factors that interfere with the assessment of the real stent lumen even on 64-slice CT. The metal of the stents can cause blooming artifacts that prevent the accurate interpretation of a lumen's patency. The blooming effect is caused by a combination of partial volume averaging and beam hardening, and this results in higher CT attenuation values in the stent lumen and this enlarges the apparent size of the stent struts, thus leading to a pseudo-narrowing of the lumen. Regarding the type of stent, the gold or gold-coated stents along with the stents made of tantalum, cause the most severe artifacts, while the stainless steel and cobalt stents can be more accurately visualized. Cardiac motion, poor contrast filling, the oblique course of the coronary vessels and calcification may also decrease the ability to assess a stent's lumen. To improve a stent's visualization, numerous methods have been attempted such as dedicated post-processing or the use of dual-source CT. However, because of its presently limited sensitivity and high radiation exposure, MDCT should not be used as the first-line test to screen for in-stent restenosis in asymptomatic patients. Given its high specificity and negative predictive value, MDCT might be valuable for confirming stent occlusion in symptomatic patients. Such stent evaluation should focus on the proximal coronary artery segments and on those stents with a diameter greater than 3 mm. (**Korean Circ J 2007;37:521-529**)

**KEY WORDS:** Multidetector row CT ; Stents ; Coronary stenosis.

## Introduction

Percutaneous coronary intervention (PCI) has gained widespread acceptance as the treatment of choice for managing symptomatic coronary disease. The most im-

portant advance in the field of PCI was the introduction of coronary stent implantation in the 1990s because this led to a reduction in both the risk of acute major complications and the incidence of restenosis, as compared with the risks after balloon angioplasty.<sup>1,2)</sup> While its technical success rate exceeds 95%, stent restenosis remains a clinical problem. The introduction of drug-eluting stents into clinical practice has dramatically reduced the occurrence of restenosis compared with the use of bare metal stents.<sup>3-5)</sup> Yet even at this low rate,

**Correspondence:** Jung Im Jung, MD, Department of Radiology, St. Mary's Hospital, College of Medicine, The Catholic University of Korea, Yeouido-dong, Yeongdeungpo-gu, Seoul 150-713, Korea  
Tel: 82-2-3779-1277, Fax: 82-2-783-5288  
E-mail: jijung@catholic.ac.kr

stent restenosis remains an important problem,<sup>6-8)</sup> and so an efficient diagnostic tool for follow up after stent placement is needed. Coronary angiography is presently the standard procedure for assessing the vessel lumen after stent placement. However, this method may involve major complications due to its invasiveness.<sup>9)</sup> Therefore, the development of noninvasive and less expensive imaging modalities to assess the patency of coronary artery stents is of great clinical interest.

Magnetic resonance (MR) angiography also can depict the coronary anatomy and it can help to detect stenosis in the proximal segments of coronary arteries.<sup>10)</sup> However, metallic stents cause magnetic susceptibility artifacts that may prevent visualization of the lumen.<sup>11)</sup> Electron-beam computed tomography (CT) has been used to assess stent patency, yet assessment with this modality depends on indirect time-attenuation analysis in the vessel segments distal to the stent, but there is no actual visualization of the in-stent lumen.<sup>12)13)</sup>

Since its introduction, the multi-detector row CT (MDCT) technology for cardiac applications has continuously evolved. With increasing the number of detector rows, CT scanners can provide markedly improved temporal and spatial resolution on coronary imaging. MDCT also allows the imaging of coronary stents. There has been a dramatic increase in the number of recent investigations that have evaluated coronary stents by MDCT, and it is now valid to ask: Is this method ready for real world clinical use?

The purpose of this article is to review the current status and perspective of MDCT imaging of coronary artery stents.

## Current Status

### Multidetector CT scanners for the visualization of coronary stents

It is generally accepted that in-stent lumen evaluation using 4-slice MDCT is impossible.<sup>14-16)</sup> An in vitro study using 4-slice MDCT to assess 19 different stents showed that reliable lumen assessment was not feasible as blooming artifacts of the metallic stents obscured significant parts of the stent lumen in most products.<sup>14)</sup> The patient studies that used 4-slice MDCT for stent assessment were similarly disappointing.<sup>14-16)</sup> Therefore, contrast enhancement in the vessel distal to the stent has to date been the best criterion for stent patency.<sup>14-16)</sup> However, observing distal run-off cannot be considered an absolute indicator of patency as the presence of vessel enhancement distal to a stent can also be secondary to retrograde filling.

The introduction of 16-slice MDCT made CT a much more viable modality for detecting significant in-stent restenosis, with reported sensitivity and specificity values in the range of 54-100% and 88-100% respectively.<sup>17-23)</sup> Coronary artery stent patency has been assessed with using 16-slice MDCT scanners on the basis of contrast enhancement measurements<sup>18-22)</sup> or pixel count methods.<sup>23)</sup> However, for stents with small (<3 mm) diameters and/or thicker struts, visualization of in-stent stenosis remains a problem.<sup>17)20)21)</sup>

The recently introduced 64-slice MDCT scanners have improved both the temporal and spatial resolutions due to their reduced rotation time and thinner sections (0.6 mm). This modality is also likely to improve CT's ability to access stents (Fig. 1, 2). In an in vitro study, using 64-slice MDCT resulted in superior visualization



**Fig. 1.** Stent (Cypher<sup>®</sup>) image with using 64-slice MDCT. A: multiplanar reformatted (MPR) image of the left coronary artery clearly demonstrates the in-stent lumen and the internal enhancing vessel (arrow). B: the cross section image demonstrates the enhancing, patent stent in the vessel. MDCT: multidetector-row CT.

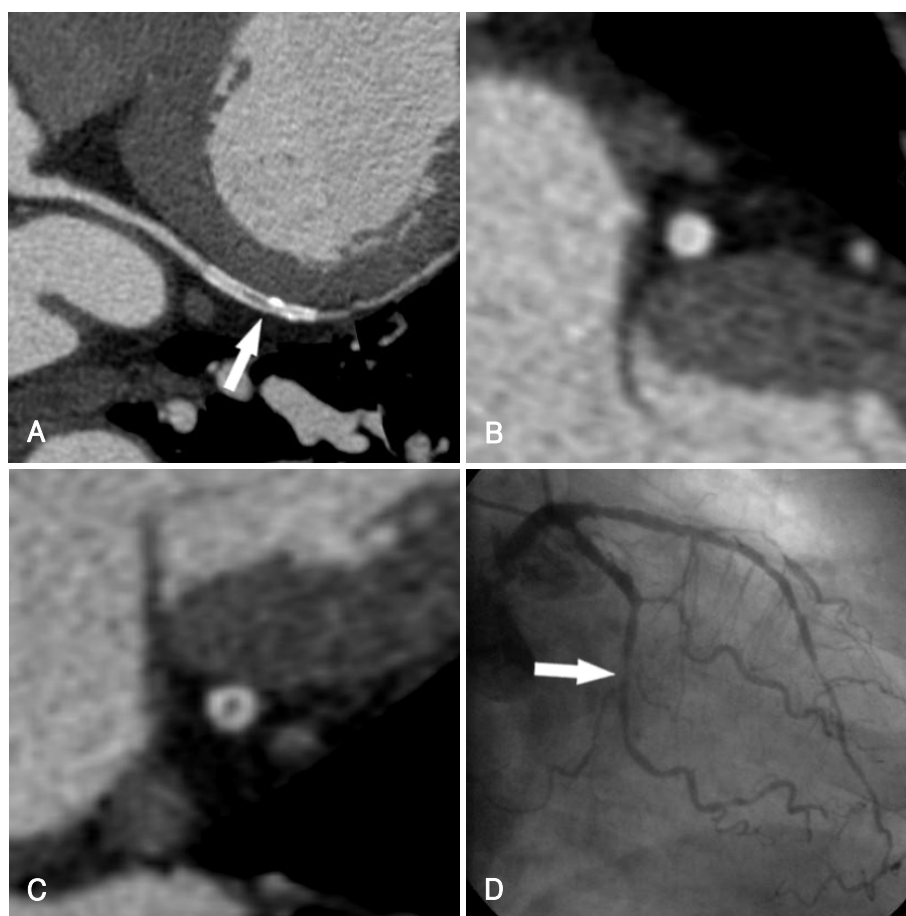


**Fig. 2.** In-stent restenosis image using 64-slice MDCT. A: the MPR image of the left circumflex artery shows lower attenuation inside the stent lumen (arrow) than that in the proximal artery. B: the cross sectional image obtained at the upper portion of the stent shows a patent enhancing vessel with an implanted stent. C: the cross sectional image obtained at the lower portion of the stent shows low attenuation within the stent, raising the possibility of in-stent occlusion. D: coronary angiography showed marked in-stent restenosis of the LCX (arrow). MDCT: multidetector-row CT, MPR: multiplanar reformatted, LCX: left circumflex artery.

of the stent lumen and in-stent stenosis compared with that of 16-slice MDCT, and especially when the stent is oriented parallel to the X-ray beam.<sup>24)</sup> The recently reported values for the sensitivity and specificity of detecting in-stent restenosis with using 64-slice MDCT are 89% and 95%, respectively.<sup>25)</sup> However, although 64-slice MDCT has allowed improved stent visualization, a relevant portion (up to 47%) of the stent lumen is still not assessable.<sup>26)</sup> There are many issues that interfere with the assessment of the real stent lumen, even with using 64-slice MDCT.

#### Issues interfering with stent assessment on Multi-detector-row CT

##### Mechanical factors (Beam hardening and the blooming effect, and the partial volume averaging effect)

Metallic stents cause a severe CT artifact known as the blooming effect; this is the result of beam hardening and it causes the stent struts to appear thicker than they really are.<sup>27)</sup> As a result the in-stent luminal diameter is underestimated. The energy spectrum of the X-ray beam

increases as it passes through a hyperattenuating structure because lower-energy photons are absorbed more rapidly than are the higher-energy photons, resulting in the beam being more intense when it reaches the detectors. Calcified spots of the vessel wall near or at the outer surface of an implanted stent also contribute to beam hardening, which further erodes the assessability of the stent lumen.<sup>28)</sup> The magnitude of the artifact varies depending on the type of metal and the stent design.<sup>29)</sup> As a rule, the depiction of stents with the slimmest profile is least affected by blooming artifacts.<sup>28)</sup> Beam hardening artifacts also may be exacerbated by motion or by inappropriate selection of the reconstruction window.<sup>30)</sup> Conversely, blooming artifacts may be minimized by reduced motion and an optimal reconstruction window.<sup>28)30)</sup>

Another mechanical obstacle to coronary stent imaging is related to the partial volume averaging effect, and this is inherent in the cross-sectional imaging modalities and it yields a CT number that represents the average attenuation of the materials within the voxel. The partial-volume averaging may affect not only the measurement

of the in-stent attenuation, but also that of the in-stent luminal diameter.<sup>29)</sup> As a result, the in-stent luminal diameters that are measured on the CT images are smaller than those measured on the conventional angiograms.<sup>22)</sup> The thin-section collimation of 64-slice MDCT and the high-resolution image post-processing algorithm help to decrease the effects of partial volume averaging.<sup>22)30-32)</sup>

### Stent type

The visibility of different stents' lumens varies and this largely depends upon the stent type and the diameter. The blooming effect is more disturbing for smaller coronary stents with thicker struts (Fig. 3). Uninterpretable images tend to be obtained for stents with thicker struts and/or a smaller diameter. When the lumen diameter is less than 3mm, the lumen visibility is worse.<sup>21)</sup> Regarding the type of stent, the most severe artifacts are found with tantalum, gold or gold-coated stents, or with covered stent grafts as compared with stainless steel stents.<sup>33)</sup> Maintz et al.<sup>34)</sup> recently evaluated 68 different stents in vitro with using 64-slice MDCT and they created a catalogue of the CT appearance of most of the currently available coronary stents (Table 1). They confirmed that the high variability for stent lumen visibility depended on the stent type, and this was previously reported on with using 4-slice and 16-slice CT. They also concluded that while in vivo studies will be required to verify their results, it can be assumed that a reliable evaluation of stents' lumens in the more advantageous stent types, such as the Radius, Teneo, Symbiot or Flex standard stents, will be possible with using 64-slice MDCT.<sup>34)</sup>

### Optimization of contrast enhancement

Optimal contrast enhancement is crucial for evaluating

stent patency as well as for evaluating coronary arteries. The acquisition time also has a major impact on the quality of vascular contrast enhancement. There are three different bolus timing techniques: fixed delay, delay estimation from a test-bolus injection and real-time bolus-tracking. While the fixed delay technique has been practically abandoned for cardiac MDCT, the bolus-tracking technique is the most commonly used method. The test-bolus technique offers the theoretical advantage of being able to prospectively plan the shape of the time-attenuation curve. This approach has the potential to improve the homogeneity of the intravascular contrast and it also allows estimation of the functional parameters.<sup>35)</sup> A high degree of intraluminal enhancement is recommended, especially for the investigation of stent patency in vessels with a small diameter and thus they contain less blood.

### Cardiac motion

Cardiac motion is one of the most important causes of vessel non-assessability on MDCT coronary angiography. The movement of coronary arteries results in blurring of the CT image and a smaller apparent stent lumen due to the partial volume effect and the metal blooming artifact. The use of high gantry rotation speeds and beta-blockers to lower the heart rate have consistently improved the interpretability of MDCT coronary angiograms.<sup>28)</sup> The use of multisegmental reconstruction (MSR) techniques could improve the image quality in patients with a high heart rate.<sup>36-38)</sup> However, Groen et al.<sup>39)40)</sup> recently reported that MSR showed no benefit of image quality for the visualization of coronary stents at high heart rates on a moving heart phantom with using 64-slice MDCT. They concluded that lowering of the heart rate is more beneficial for image quality than using a



**Fig. 3.** Variations of the severity of metal-related artifacts seen on 64-slice MDCT with variations of the metallic contents, the design and the luminal diameter of the stent. A: the MPR image shows two different stents in the LAD. Note the stent in the proximal LAD (Express<sup>®</sup>) shows more pronounced metal-related artifact than does the distal stent (Tetra<sup>®</sup>). B: cross section image of the proximal stent (Express<sup>®</sup>: 0.13 mm for the strut thickness). C: cross section image of the distal stent (Tetra<sup>®</sup>: 0.09–0.12 mm for the strut thickness). MDCT: multidetector-row CT, MPR: multiplanar reformatted, LAD: left anterior descending artery.

**Table 1.** The commercial name, the manufacturer and material, the struts dimensions and the percent of the mean diameters of the visible stent lumen on 64-slice CT (Modified from the tables of Maintz et al.<sup>34)</sup> with permission)

No.	Name	Manufacturer	Material	Diameter (mm)	Length (mm)	Strut thickness (mm)	Visible diameter on CT (%)
1	ACS Multilink	Guidant	Stainless steel 316L	3	25	0.127	56.70
2	Arthos-Inert	AMG International	Stainless steel 316L	3	24	0.105	63.30
3	Arthos-Pico	AMG International	Cobalt-chromium alloy	3	18	0.074	66.70
4	be-Stent 2	Medtronic	Stainless steel 316L	3	10	0.102-0.109	53.30
5	Biodiv Ysio	Abbott Vascular Devices	Stainless steel 316L+ Phosphorylcholine coating	3	19	0.091	63.30
6	CCSV	Micro Science Medical	Stainless steel 316L, Tantal coating	3	16	0.6-0.8	60.00
7	Coroflex	B. Braun	Stainless steel 316L	3	25	0.100	63.30
8	Coroflex Blue	B. Braun	Cobalt-chromium alloy (L605)	2.5	16	0.065	53.30
9	Coroflex Delta	B. Braun	Stainless steel 316L	3.5	16	0.120	60.00
10	Crossflex	Cordis	Stainless steel 316L	3	22	0.152	60.00
11	CSG (R010F26)	Abbott Vascular Devices	Stainless steel 316L	3	24	0.3	56.70
12	Cypher	Cordis	Stainless steel 316L	3	13	0.14	56.70
13	Driver	Medtronic	Cobalt-chromium alloy	3	18	0.097	66.70
14	Duett	Guidant	Stainless steel 316L	3	7	0.14	46.70
15	Express 2	Boston scientific	Stainless steel 316L	4	20	0.13	50.00
16	F1 Large (010FF12)	Abbott Vascular	Stainless steel 316L	3	12	0.09	63.30
17	F1 Medium (009FF12)	Devices	Stainless steel 316L	2.75	12	0.09	63.30
18	F1 Small (006FF16)	Abbott Vascular Devices	Stainless steel 316L	2.5	15	0.09	63.30
19	Flex AS	Phytis	Stainless steel 316L+ DLC coating	3	7	0.09	53.30
20	Flex Small (006F26)	Abbott Vascular Devices	Stainless steel 316L	2.5	26	0.09	66.70
21	Flex Standard (010F12)	Phytis	Stainless steel 316L	3	12	0.09	70.00
22	Herculink	Guidant	Stainless steel 316L	4	18	0.102-0.109	40.00
23	Jograft	Abbott Vascular Devices	Stainless steel 316L+ PTFE-graft	3	9	0.091-0.124	56.70
24	Jostent	Abbott Vascular	Stainless steel 316L	3	19	0.09	56.70
25	Lekton	Devices	Stainless steel 316L, Silicon-carbide coating	2.75	15	0.8-1.0	60.00
26	Liberté	Boston Scientific	Stainless steel 316L+PTFE	3	20	0.096	53.30
27	MAC	AMG International	Stainless steel 316L	3	13	0.120	63.30
28	Magic Wallstent	Bostone Scientific	Cobalt alloy with titanium core (33%)	4	32	0.1	
29	Mansfield Coronary Stent	Mansfield	Tantalum	3.5	20	0.1	23.30
30	MicroStent	Medtronic-AVE	Stainless steel 316L	3.5	4	0.1	36.70
31	Mini	Cordis	Stainless steel 316L	3	28	0.1	56.70
32	MSM Coronary Stent	Micro Science Medical	Stainless steel 316L, Tantal coating	3	26	0.08	60.00
33	Nexus	Occam International	Stainless steel 316L	3	19	0.11-0.13	60.00
34	Nexus 2	Occam International	Stainless steel 316L	3	15	0.11-0.13	66.70
35	NIR Primo	Bostone Scientific	Stainless steel 316L	3	32	0.091-0.124	56.70
36	NIR Royal	Bostone Scientific	Stainless steel 316LS+ gold coating	3	25	0.14	33.00
37	NIR Royal Adv	Bostone Scientific	Stainless steel 316LS+ gold coating	3.5	15	0.11	43.30
38	Palmaz	Cordis	Stainless steel 316L	3	14	0.07-0.095	53.30
39	Palmaz-Crown	Cordis	Stainless steel 316L	3	22	0.091	53.30

Table 1. Continued

No.	Name	Manufacturer	Material	Diameter (mm)	Length (mm)	Strut thickness (mm)	Visible diameter on CT (%)
40	Penta	Guidant	Stainless steel 316L	3.5	15	0.09-0.12	60.00
41	Pixel	Guidant	Stainless steel 316L	2.5	23	0.1	50.00
42	Radius	Boston	Nitinol	3	20	0.08-0.09	73.30
43	Rithron-XR	Biotronik	Stainless steel 316L	2.5	30	0.08	50.00
44	R-Stent	Orbuts Medical Technologies	Stainless steel 316L	3	25	0.1-0.127	63.30
45	S7	Medtronic	Stainless steel 316L	4	15	0.102-0.128	66.70
46	Sirius Carbostent	Sorin Biomedica	Stainless steel 316L+carbon coating+2 Platinum markers	3	15	0.091-0.124	53.30
47	Sito Stents	Sitomed	Stainless steel 316L	2.5	28	0.1	50.00
48	Sonic Bx	Cordis	Stainless steel 316L	2.5	18	0.14	46.70
49	Symbiot	Boston Scientific	Nitinol	4	20	0.110	70.00
50	Syncro	Sorin Biomedica	Stainless steel 316L+carbon coating+2 Platinum markers	3	19	0.075	53.30
51	Tantal	Abbott Vascular Devices	Tantalum-based alloy	3.5	5	0.08	30.00
52	Tantal Sandwich	Abbott Vascular Devices	316L (inside), Ta (intermediate), 316L (outside)	3	18	0.07	46.70
53	Taxus	Boston Scientific	Stainless steel 316L	3.5	12	0.13	56.70
54	Tecnic	Sorin Biomedica	Stainless steel 316L+carbone coating+2 Platinum markers	3	19	0.075	53.30
55	Tenax-complete	Biotronik	Stainless steel 316L	3.5	15	0.08	66.70
56	Tenax-XR	Biotronik	Stainless steel 316L, gold markers	3	15	0.08	63.30
57	Teneo	Biotronik	Stainless steel 316L	4	10	0.08	70.00
58	Tetra	Guidant	Stainless steel 316L	3	13	0.09-0.12	53.30
59	Tristar	Guidant	Stainless steel 316L	4	18	0.102-0.109	53.30
60	Tsunami	Terumo	Stainless steel 316L	3	30	0.08	56.70
61	Tsunami Gold	Terumo	Stainless steel 316L	3	10	0.08	60.00
62	Ultra	Guidant	Stainless steel 316L	3.5	18	0.128	53.30
63	Velocity Bx	Cordis	Stainless steel 316L	3	18	0.14	60.00
64	V-Flex Plus	Cook	Stainless steel 316L	3	12	0.069	56.70
65	Vision	Guidant	Cobalt-chromium alloy	3	15	0.81	66.70
66	Wallstent	Boston Scientific	Stainless steel 316L	5	35	0.1	63.30
67	Wiktor	Medtronic	Tantalum	3.5	30	0.064	3.30
68	Zeta	Guidant	Stainless steel 316L	3	18	0.09-0.12	53.30

MSR technique. They also reported that in order to reduce blurring, it is more efficient to reduce the heart rate than to increase the temporal resolution.<sup>40)</sup>

#### Anatomical factors

The coronary arteries typically have an oblique course and they are often assessed from multiplanar reformats of the axial images. Therefore, all the stents are positioned at two different angles towards the z-axis of the MDCT scanner in order to simulate different scenarios regarding the spatial resolution along the z-axis.<sup>26)</sup> Mahnken et al.<sup>31)</sup> have investigated a small series of different stents at orientations of 0°, 45° and 90° toward the z-axis with using 16-slice CT, and they found that 0° was the most advantageous orientation. This may be the most likely orientation of a stent in the mid-segment of the right coronary

artery. Stents in other vessels have decreased spatial resolution along the z-axis, which indicates that the assessable inner stent lumen is decreased. However, with the thinner slices of 64-slice CT, the orientation of 90° toward the z-axis could lead to better performance.<sup>24)</sup>

Another patient factor that might limit proper assessment of stent lumens, as well as the native coronary artery lumens, is severe calcification, and this should also be mentioned (Fig. 4). Ohnuki et al.<sup>23)</sup> evaluated coronary in-stent stenosis on 16-slice MDCT. Of the 20 lesions, two cases were misinterpreted due to calcification. Because of the calcification artifact, it is difficult to identify contrast in the lumen. Any calcification in the proximal portion of the left anterior descending artery is most likely to be severe and it is most influential on the assessability of the stents implanted in segment #6.<sup>21)</sup> However, as

the severity and distribution of calcification are not uniform, these factors affect every stent in the other segments of the coronary arteries that have calcification and so this is considered to be one of the limitations of the currently available MDCT.

## Perspective

### How to overcome the limitations of Multidetector-row CT for the imaging of coronary stents

#### Dedicated edge-enhancing convolution kernel

Post-processing is an important part of lumen visualization of a coronary stent. An edge-enhancing, high-spatial-resolution kernel for reconstruction yields fewer blooming artifacts and less artificial lumen narrowing, and the intraluminal attenuation changes caused by such artifacts would therefore be minimized.<sup>41-44</sup> Maintz et al.<sup>41</sup> reported an average 23% increase in the visible lumen diameter and a mean reduction of the intraluminal attenuation of roughly 30% when they used the edge-enhancing, high-spatial resolution kernel (B45f convolutional kernel). Mahnken et al.<sup>42</sup> found significantly smaller artificial lumen narrowing and lower intraluminal attenuation when they used a B45f convolutional kernel, as compared to the smoother B30f kernel. While the B45f convolution kernel is optimized to reduce the blooming artifacts that occur at the edges of structures that have high attenuation values, such as calcified plaques or metallic structures, a significant increase in image noise must be accepted as a trade-off, although this reduces the overall image quality and hampers the delineation of small low-contrast structures.<sup>41-44</sup>

#### Stents

As was discussed above, the most severe artifacts are found with tantalum, gold or gold-coated stents, or with covered stents grafts as compared with stainless steel stents. Stents with lesser artifacts should be selected when follow up is planned. In the future, the development of CT transparent stents or biodegradable stents may create optimal conditions for non-invasive post-implantation follow-up with using MDCT.

#### Dual-source spiral CT

Residual cardiac motion has a role in increasing the metal-related artifacts such as beam hardening and partial volume averaging effects. Dual-source spiral CT (DSCT) provides a temporal resolution of 83 milliseconds (165 milliseconds on 64-slice MDCT). Lell et al.<sup>45</sup> recently evaluated coronary stents and stenoses at different heart rates in vitro. They concluded that the depiction of coronary stents with DSCT is possible across a large range of simulated heart rates (50-120 bpm) without incurring motion artifacts. The overall measurement errors of the in-stent diameter with using DSCT were markedly smaller than those reported for 16-slice MDCT and they were smaller than those reported for 64-slice MDCT. Although larger clinical studies will be necessary to establish the accuracy of DSCT for assessing the degree of coronary artery stenosis in vivo, the preliminary results seems to be quite promising.

## Conclusion

MDCT has recently emerged as a noninvasive method for evaluating coronary stents. Because of its presently

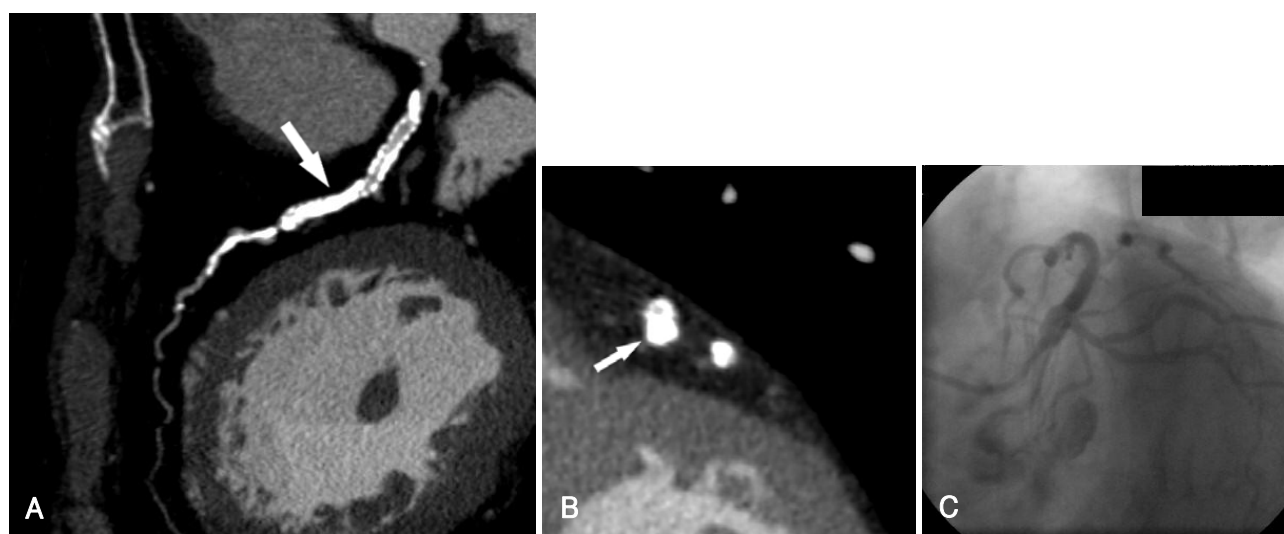


**Fig. 4.** Calcification hampers visualization of the in-stent lumen. A: continued stents at the proximal and mid LAD. Note the extensive calcifications at the stent of the mid LAD (arrow) prohibit the visualization of the in-stent lumen. B: the cross sectional image shows that calcification at the outer edge of the stent of the mid LAD contributes to beam hardening and this hampers visualization of the in-stent lumen. C: coronary angiography shows a patent LAD without any in-stent stenosis. LAD: left anterior descending artery.

limited sensitivity due to the various factors discussed above and because of its high radiation exposure, MDCT should not yet be used as a first-line test to screen for in-stent restenosis in asymptomatic patients. However given its high specificity and negative predictive value, MDCT might be valuable for confirming stent occlusion in symptomatic patients. Stent evaluation should focus on the proximal coronary artery segments and on stents with a diameter greater than 3 mm. Ideally the stent type should be known prior to the scan, as assessment of a particular type of stent can be predicted from in vitro-data. Larger clinical studies and further technical advances will be needed in the future to optimize the utility of MDCT for assessing the lumens in stents and in the coronary arteries.

### Acknowledgments

I want to thank Yun Seok Choi, MD, for his kind help in the preparation of the manuscript. Also I wish to thank Bonnie Hami, MA (USA) for her editorial assistance with the preparation of the manuscript.

### REFERENCES

- Serruys PW, de Jaegere P, Kiemenenij F, et al. *A comparison of balloon-expandable-stent implantation with balloon angioplasty in patients with coronary artery disease.* *N Engl J Med* 1994;331:489-95.
- Fischman DL, Leon MB, Baim DS, et al. *A randomized comparison of coronary-stent placement and balloon angioplasty in the treatment of coronary artery disease.* *N Engl J Med* 1994;331:496-501.
- Moses JW, Leon MB, Popma JJ, et al. *Sirolimus-eluting stents versus standard stents in patients with stenosis in a native coronary artery.* *N Engl J Med* 2003;349:1315-23.
- Hong YJ, Jeong MH. *New drug-eluting stents.* *Korean Circ J* 2005;35:197-205.
- Whang Y, Kim H, Kim K, et al. *The efficacy of drug eluting stents on restenosis reduction in small coronary arteries.* *Korean Circ J* 2006;36:450-7.
- Park SH, Hong GR, Seo HS, Tahk SJ. *Stent thrombosis after successful drug-eluting stent implantation.* *Korean Circ J* 2005;35:163-71.
- Lim DS. *Coronary restenosis after drug-eluting stent implantation in diabetic patients.* *Korean Circ J* 2006;36:1-7.
- Lee CW, Park S. *Predictive factors for restenosis after drug-eluting stent implantation.* *Korean Circ J* 2007;37:97-102.
- Scanlon PJ, Faxon DP, Audet AM, et al. *ACC/AHA guidelines for coronary angiography: a report of the American College of Cardiology/American Heart Association Task Force on practice guidelines (Committee on Coronary Angiography): developed in collaboration with the Society for Cardiac Angiography and Interventions.* *J Am Coll Cardiol* 1999;33:1756-824.
- Kim WY, Danias PG, Stuber M, et al. *Coronary magnetic resonance angiography for the detection of coronary stenoses.* *N Engl J Med* 2001;345:1863-9.
- Hug J, Nagel E, Bornstedt A, Schnackenberg B, Oswald H, Fleck E. *Coronary arterial stents: safety and artifacts during MR imaging.* *Radiology* 2000;216:781-7.
- Pump H, Mohlenkamp S, Sehnert CA, et al. *Coronary arterial stent patency: assessment with electron-beam CT.* *Radiology* 2000;214:447-52.
- Knollmann FD, Moller J, Gebert A, Bethge C, Felix R. *Assessment of coronary artery stent patency by electron-beam CT.* *Eur Radiol* 2004;14:1341-7.
- Maintz D, Grude M, Fallenberg EM, Heindel W, Fischbach R. *Assessment of coronary arterial stents by multislice-CT angiography.* *Acta Radiol* 2003;44:597-603.
- Kruger S, Mahnken AH, Sinha AM, et al. *Multislice spiral computed tomography for the detection of coronary stent restenosis and patency.* *Int J Cardiol* 2003;89:167-72.
- Ligabue G, Rossi R, Ratti C, Favali M, Modena MG, Romgnoli R. *Noninvasive evaluation of coronary artery stents patency after PTCA: role of multislice computed tomography.* *Radiol Med* 2004;108:128-37.
- Schuijf JD, Bax JJ, Jukema JW, et al. *Feasibility of assessment of coronary stent patency using 16-slice computed tomography.* *Am J Cardiol* 2004;94:427-30.
- Cademartiri F, Mollet N, Lemos PA, et al. *Usefulness of multislice computed tomographic coronary angiography to assess in-stent restenosis.* *Am J Cardiol* 2005;96:799-802.
- Gilard M, Cornily JC, Rioufol G, et al. *Noninvasive assessment of left main coronary stent patency with 16-slice computed tomography.* *Am J Cardiol* 2005;95:110-2.
- Gilard M, Cornily JC, Pennec PY, et al. *Assessment of coronary artery stenosis by 16-slice computed tomography.* *Heart* 2006;92:58-61.
- Kitagawa T, Fujii T, Tomohiro Y, et al. *Noninvasive assessment of coronary stents in patients by 16-slice computed tomography.* *Int J Cardiol* 2006;109:188-94.
- Hong C, Chrysanti GS, Woodard PK, Bae KT. *Coronary artery stent patency assessed with in-stent contrast enhancement measured at multi-detector row CT angiography: initial experience.* *Radiology* 2004;233:286-91.
- Ohnuki K, Yoshida S, Ohta M, et al. *New diagnostic technique in multi-slice computed tomography for in-stent restenosis: pixel count method.* *Int J Cardiol* 2006;108:251-8.
- Seifarth H, Ozgun M, Raupach R, et al. *64-versus 16-slice CT angiography for coronary artery stent assessment: in vitro experience.* *Invest Radiol* 2006;41:22-7.
- Oncel D, Oncel G, Karaca M. *Coronary stent patency and in-stent restenosis: determination with 64-section multidetector CT coronary angiography-initial experience.* *Radiology* 2007;242:403-9.
- Mahnken AH, Muhlenbruch G, Seyfarth T, et al. *64-slice computed tomography assessment of coronary artery stents: a phantom study.* *Acta Radiol* 2006;47:36-42.
- Nieman K, Cademartiri F, Raaijmakers R, Pattynama P, de Feyter P. *Noninvasive angiographic evaluation of coronary stents with multi-slice spiral computed tomography.* *Herz* 2003;28:136-42.
- Pugliese F, Cademartiri F, van Mieghem C, et al. *Multidetector CT for visualization of coronary stents.* *Radiographics* 2006;26:887-904.
- Maintz D, Juergens KU, Wichter T, Grude MJ, Heindel W, Fischbach R. *Imaging of coronary artery stents using multislice computed tomography: in vitro evaluation.* *Eur Radiol* 2003;13:830-5.
- Choi HS, Choi BW, Choe KO, et al. *Pitfalls, artifacts, and remedies in multi-detector row CT coronary angiography.* *Radiographics* 2004;24:787-800.
- Mahnken AH, Seyfarth T, Flohr T, et al. *Flat-panel detector computed tomography for the assessment of coronary artery stents: phantom study in comparison with 16-slice spiral computed tomography.* *Invest Radiol* 2005;40:8-13.
- Nieman K, Cademartiri F, Lemos PA, Raaijmakers R, Pattynama PM, de Feyter PJ. *Reliable noninvasive coronary angiography with fast submillimeter multislice spiral computed tomography.* *Circulation* 2002;106:2051-4.

- 33) Mahnken AH, Buecker A, Wildberger AJ, et al. *Coronary artery stents in multislice computed tomography: in vitro artifact evaluation. Invest Radiol* 2004;39:27-33.
- 34) Maintz D, Seifarth H, Raupach R, et al. *64-slice multidetector coronary CT angiography: in vitro evaluation of 68 different stents. Eur Radiol* 2006;16:818-26.
- 35) Mahnken AH, Muhlenbruch G, Gunther RW, Wildberger JE. *Cardiac CT: coronary arteries and beyond. Eur Radiol* 2007;17:994-1008.
- 36) Flohr T, Kuttner A, Bruder H, et al. *Performance evaluation of a multi-slice CT system with 16-slice detector and increased gantry rotation speed for isotropic submillimeter imaging of the heart. Herz* 2003;28:7-19.
- 37) Greuter MJ, Dorgelo J, Tukker WG, Oudkerk M. *Study on motion artifacts in coronary arteries with an anthropomorphic moving heart phantom on an ECG-gated multidetector computed tomography unit. Eur Radiol* 2005;15:995-1007.
- 38) Juergens KU, Maintz D, Grude M, et al. *Multi-detector row computed tomography of the heart: does a multisegment reconstruction algorithm improve left ventricular volume measurements? Eur Radiol* 2005;15:111-7.
- 39) Groen JM, Greuter MJ, van Ooijen PM, Willems TP, Oudkerk M. *Initial results on visualization of coronary artery stents at multiple heart rates on a moving heart phantom using 64-MDCT. J Comput Assist Tomogr* 2006;30:812-7.
- 40) Groen JM, Greuter MJ, van Ooijen PM, Oudkerk M. *A new approach to the assessment of lumen visibility of coronary artery stent at various heart rates using 64-slice MDCT. Eur Radiol* 2007;17:1879-84.
- 41) Maintz D, Seifarth H, Flohr T, et al. *Improved coronary artery stent visualization and in-stent stenosis detection using 16-slice computed tomography and dedicated image reconstruction technique. Invest Radiol* 2003;38:790-5.
- 42) Mahnken AH, Buecker A, Wildberger JE, et al. *Coronary artery stents in multislice computed tomography: in vitro artifact evaluation. Invest Radiol* 2004;39:27-33.
- 43) Seifarth H, Raupach R, Schaller S, et al. *Assessment of coronary artery stents using 16-slice MDCT angiography: evaluation of a dedicated reconstruction kernel and a noise reduction filter. Eur Radiol* 2005;15:721-6.
- 44) Schepis T, Koepfli P, Leschka S, et al. *Coronary artery stent geometry and in-stent contrast attenuation with 64-slice computed tomography. Eur Radiol* 2007;17:1464-73.
- 45) Lell MM, Panknin C, Saleh R, et al. *Evaluation of coronary stents and stenoses at different heart rates with dual source spiral CT (DSCT). Invest Radiol* 2007;42:536-41.